Innovative Systems Design and Engineering
ISSN 2222-1727 (Paper) ISSN 2222-2871 (Online)
Vol 2, No 3
www.iiste.org

Transient analysis of grid-connected wind-driven PMSG, DFIG and SCIG at fixed and variable speeds

Mazen Abdel-Salam (Corresponding author)
Electric Engineering Department, Assiut University, Assiut, Egypt
E-mail: mazen2000as@yahoo.com

Adel Ahmed
Electric Engineering Department, Assiut University, Assiut, Egypt
E-mail: a_ahmed@aun.edu.eg

Mahmoud Mahrous
Electric Engineering Department, Assiut University, Assiut, Egypt
E-mail: mahmoud2006eng@yahoo.com

Abstract

This paper is aimed at presenting transient analysis of a grid-connected wind-driven permanent magnet synchronous generator (PMSG) at fixed and variable speeds by solving the system describing differential equations. For comparison purpose, wind-driven squirrel cage (SCIG) and doubly fed (DFIG) induction generators at fixed and variable speeds are studied using MATLAB/SIMULINK software package. Different from PMSG and DFIG the grid should feed the reactive losses of transmission lines and transformers at any value of short circuit ratio for SCIG. This increases the dynamic stability of DFIG and PMSG when compared with SCIG. Under three-phase-to-ground fault and single-phase-to-ground fault conditions, the time required to recover stability of PMSG wind farm is less than those DFIG and SCIG wind farms for fixed and variable speeds indicating that PMSG is more stable than of DFIG and of SCIG wind farms.

Keywords: Wind energy; Fixed and variable speed wind turbine; Permanent magnet synchronous generator; Induction generator; Short circuit ratio.

1. Introduction

Wind turbine technology has undergone a dramatic transformation during the last 15 years, developing from a fringe science in the 1970s to the wind turbines of the 2000s utilizing the latest technology in power electronics, aerodynamics and mechanical drive designs.

Induction generators are more attractive than synchronous generators for wind turbines due to their robust construction, low cost, low maintenance, long life (more than 50 years) and low power to weight ratio (Bhadra 2005). However the reactive power management is a major concern, not only to compensate for the reactive power requirements of the wind generator itself but also to support the system voltage in particular for wind farms based on fixed speed induction generators.

Most wind turbines use induction generators, squirrel cage induction generator (SCIG), doubly-fed-induction-generators (DFIG) or permanent magnet synchronous generators (PMSG). Currently, DFIG based wind turbines dominate the world market due to their cost-effective provision of variable-speed operation, as well as the controlling flexibility of electromagnetic torque and reactive power. However, since its stator and rotor are both connected to the power system, grid fault ride-through control (on temporal reduction of the grid voltage due to a fault) is difficult for the DFIG, and is a major challenge for wind turbine manufacturers based on the MATLAB/SIMULINK without stating the system describing equations (Zhanfeng 2010). In the existing literature, there have recently been several papers dealing with this problem, mainly focusing on ride-through controller design and transient response analysis based on the system describing equations after being linearized and models the state variables of the original system states from the nominal operating values (Rahim 2011).

The analysis of a configuration consisting wind farm based on conventional fixed speed SCIG has been reported before (Fischer de Toledo 2005). Improvement of the short-term voltage and rotor stability performance on introducing a STATCOM was quantified during different types of failure events in the connected power system (three-phase to ground fault and single-phase to ground fault) using EMTDC/PSCAD digital simulator. Also, the effect of electrical parameters of the induction generator on the transient voltage stability of a fixed speed wind turbine (FSWT) connected to a simple grid based on the MATLAB/SIMULINK (Dusonchet 2011).

When compared with induction generators, the PMSG has a smaller physical size and a lower moment of inertia which means a higher reliability and power density per volume ratio. The electrical losses in the rotor are eliminated on the expense of high costs for permanent magnet materials and fixed excitation, which cannot be changed according to the operating point. The model used in this study was developed in the d-q synchronous rotating reference frame (Kesraoui 2010). PMSG based direct driven turbine is connected to the grid by through AC- DC- AC conversion system, modeled and simulated using MATLAB/SIMULINK (Mittal 2008).

This paper is aimed at presenting a transient analysis model of a grid-connected wind-driven permanent magnet synchronous generator (PMSG) at fixed and variable speeds by solving the system describing differential equations. The PMSG is the equivalent generator of many wind-driven synchronous generators operating in a wind farm. For comparison purpose, wind-driven squirrel cage (SCIG) and doubly fed (DFIG) induction generators running at fixed and variable speeds are studied using MATLAB/SIMULINK.

Different line connections between the grid and the wind farm with subsequent different short-circuit ratios are studied. The study extends to include three-phase-to-ground and single-phase-to-ground faults at the point where the wind farm is connected to the grid. The time required for the wind farm to recover stability is assessed for wind driven PMSG, DFIG and SCIG.

2. Network

There are a number of possible interconnection structures for wind farms and thus it is not possible to cover every type of network configuration, load, and interconnection point of the wind farm. Frequently wind parks are connected to weak systems, as they are typically located far from major load centers and central generation. This reflects itself in defining a short circuit ratio (SCR) of the interconnection expressed as:

$$SCR = \frac{SCC}{S_{base}} \tag{1}$$

Where S_{base} is the rated power of wind farm and SCC or short circuit capacity is the short circuit power delivered from the grid to a three-phase fault at the wind farm:

$$SCC = \frac{V_{base}^2}{|Z_{line}|} \tag{2}$$

where Z_{line} is the impedance of the line connecting the grid with wind farm and V_{base} is the rated voltage of the grid. For weak systems the SCR will usually be less than 6 (Abbey 2005).

3. System modeling

3.1 Grid-connected Wind-driven Permanent Magnet Synchronous Generator (PMSG) System

The block diagram of the system is shown in fig. 1. The system consists of wind-driven PMSG, an AC-DC three phase bridge rectifier, DC-DC boost converter to fixed the voltage at certain specified value and PWM inverter to interface the system with the electric utility.

3.1.1 PMSG Modeling

The PMSG is described by the following differential equations (Hong-Woo 2010) and (Whei-Min 2011):

$$\frac{1}{\omega_b}\frac{d\psi_{ds}}{dt} = v_{ds} + R_s i_{ds} + \omega_e \psi_{qs}$$
$$\frac{1}{\omega_b}\frac{d\psi_{qs}}{dt} = v_{qs} + R_s i_{qs} - \omega_e \psi_{ds} \quad (3)$$

With

$$\psi_{ds} = -L_{ds} i_{ds} - \psi_m$$
$$\psi_{qs} = -L_{qs} i_{qs} \quad (4)$$

where v is the p.u voltage, R_s is the p.u resistance, i is the p.u current, ω_e is the p.u stator electrical angular speed, ω_b is the base angular speed in rad/s, L_s is the p.u stator leakage inductance, ψ_m is the p.u exciter flux of the PMSG, and ψ is the p.u flux linkage. The subscripts d and q indicate the direct and quadrature axis components, respectively. The subscripts s indicates stator quantities. The electrical active and reactive power delivered by the stator are given by

$$P_s = v_{ds} i_{ds} + v_{qs} i_{qs}$$
$$Q_s = v_{ds} i_{qs} - v_{qs} i_{ds} \quad (5)$$

The voltages of phases d, q and 0 are transformed by Park's transformation (P) to a, b and c variables as follows (Grainger 1994):

$$\begin{bmatrix} v_a \\ v_b \\ v_c \end{bmatrix} = P^{-1} \begin{bmatrix} v_d \\ v_q \\ v_0 \end{bmatrix} \quad (6)$$

$$P = \sqrt{\frac{2}{3}} \begin{bmatrix} \cos\theta_d & \cos(\theta_d - 120) & \cos(\theta_d + 120) \\ \sin\theta_d & \sin(\theta_d - 120) & \sin(\theta_d + 120) \\ \frac{1}{\sqrt{2}} & \frac{1}{\sqrt{2}} & \frac{1}{\sqrt{2}} \end{bmatrix} \quad (7)$$

3.1.2 Uncontrolled rectifier and DC-DC boost converter

As the wind speed is constantly varying so the PMSG produces variable voltage and variable frequency output. A three-phase uncontrolled diode rectifier is used to convert the PMSG output AC voltage to DC voltage. The rectifier output voltage (Vdc) depends on the AC line voltage as expressed (Mohan 1989):

$$V_{dc} = \frac{3\sqrt{3}}{\pi} V_m = \frac{3\sqrt{2}}{\pi} V_{LL} \quad (8)$$

Where V_m is the maximum phase voltage and V_{LL} is the rms value of the line-line voltage.

As the PMSG voltage is variable with the wind speed, the DC output voltage of the bridge rectifier is also variable. A boost DC-DC converter has been used for maintaining the DC output voltage at constant value V_{do}. The relation between the

output and input voltages depends on the duty ratio D as expressed by equations (9) and (10), where T_s is the switching period and ton is the on time of the switch, the switch mode DC-DC converter signal is generated by compared the triangular wave (its period Ts) with DC wave as shown in fig. 2 (Mohan 1989).

$$\frac{V_{do}}{V_{dc}} = \frac{1}{1-D} \tag{9}$$

$$D = \frac{t_{on}}{T_s} \tag{10}$$

The control block diagram consists of a comparator, which compares the actual DC-DC converter output with a reference value. The error signal is fed to a PI controller passes though a limiter within the controller. The output of the PI controller used to generate the switching signal.

3.1.3 PWM Inverter

The inverter inverts the DC voltage output to AC voltage with supply frequency in order to connect the wind-driven system to the grid. The output of the PWM inverter (Mohan 1989) may be expressed as:

$$V_{LL1} = \frac{\sqrt{3}}{2\sqrt{2}} m_a V_{do} = 0.612 m_a V_{do} \tag{11}$$

$$m_a = \frac{\hat{V}_{control}}{\hat{V}_{tri}} = \frac{\hat{V}_{LL}}{V_{do}} \tag{12}$$

$$m_f = \frac{f_s}{f_1} \tag{13}$$

Where m_a called the modulation index, $\hat{V}_{LL}$ is the peak value of the line-line voltage, V_{LL1} is the fundamental component in the output voltage, $\hat{V}_{tri}$ is the peak amplitude of the triangular which is kept constant, $\hat{V}_{control}$ is the peak amplitude of the control signal, m_f is the frequency modulation ratio, f_s is the switching frequency and f_1 is the fundamental component frequency. It is always desirable to minimize the distortion of the output voltage and current, which change with the modulation index in linear modulation ($m_a \leq 1.0$) and over-modulation region ($m_a > 1$). In the linear region ($m_a \leq 1.0$) the fundamental- frequency component in the output voltage varies linearly with the amplitude modulation ratio m_a as expressed by equation (12). Also, the harmonics in the inverter output voltage waveform appear as sidebands, centered around the switching frequency referred to the fundamental and its multiples, that is, around harmonics m_f, 2 m_f, 3 m_f, and so on (Mohan 1989).

3.1.4 Modeling of grid-connected wind-driven PMSG system using Runge- Kutta Method

The PMSG wind farm connected to a grid is modeled by solving the describing differential equations using runge-kutta method (Sermutlu 2004) as described by the flow chart of fig. 3.The solution ends up with the temporal variation of the currents, voltages and active and reactive power.

3.2 Grid-connected Wind-driven Squirrel Cage Induction Generator (SCIG) System

In wind-driven SCIG, the stator winding is connected directly to the grid and the rotor is driven by the wind turbine as shown in fig. 4. The power captured by the wind turbine is converted into electrical power by the induction generator and is transmitted to the grid by the stator winding. The pitch angle is controlled in order to limit the generator output power to its nominal value at high wind speeds. In order to generate power, the induction generator speed must be slightly above the synchronous speed. The reactive power absorbed by the induction generator is provided by the grid or by some devices like capacitor banks, SVC, STATCOM or synchronous condenser (Mathworks 2008a). The present transient analysis of the system is based on MATLAB/SIMULINK simulation for fixed and variable wind speeds.

3.3 Grid-connected Wind-driven Doubly Fed Induction Generator (DFIG) system

In wind-driven doubly-fed induction generator (WTDFIG), Fig. 5 an AC/DC/AC converter connects the rotor of the generator to the grid. The AC/DC/AC converter is divided into two components: the rotor-side converter (CON_{rotor}) and the grid-side converter (CON_{grid}).CON_{rotor} and CON_{grid} are Voltage-Sourced Converters that use forced-commutated IGBTs to synthesize an AC voltage from a DC voltage source. The synthesized AC voltage is of power frequency for CON_{grid} and of slip frequency for CON_{rotor}. A capacitor connected on the DC side acts as the DC voltage source. A coupling inductor L is used to connect CON_{grid} to the grid. The three-phase rotor winding is connected to $CON_{rotor}$by slip rings and brushes and the three-phase stator winding is directly connected to the grid. The power captured by the wind turbine is converted into electrical power by the induction generator and transmitted to the grid by the stator and the rotor windings. The control system generates pitch angle and voltage command signals Vr and Vgc for CON_{rotor} and CON_{grid} respectively in order to control the wind turbine power comparison against a reference power obtained from the tracking characteristic. A Proportional-Integral (PI) regulator is used to reduce the power error to zero, while adjusting the DC bus voltage and the reactive power or the voltage at the grid terminals (Mathworks 2008a). Similar to SCIG system, the present transient analysis of the DFIG system is based also on MATLAB/SIMULINK simulation for fixed and variable wind speeds.

4. Grid-Connected Wind-driven Systems under study

The one line diagram of the test system employed in this study is shown in Fig. 6 for different types of wind farm.

The wind farm of PMSG consists of 75 units of 1.6 MVA wind turbines. Each wind turbine unit consists of: rotor, gear box, permanent magnet synchronous generator, uncontrolled converter, DC-DC boost converter, inverter and a 0.69/10.5 kV transformer as shown in fig. 6a. In the wind farm of SCIG, each wind turbine unit is the same as in PMSG in addition to shunt capacitors for reactive power compensation, but without uncontrolled converter, DC-DC boost converter and inverter as shown in fig. 6b. In the wind farm of DFIG, each wind turbine unit is the same as that of PMSG as shown in fig. 6c. In The representation of the power plant has been made by aggregating all the 75 wind turbines in one equivalent unit. Phase model is used for wind turbine induction generator (SCIG) and doubly fed induction generator (DFIG) systems (El-Helw 2008).

5. Simulation studies

The grid-connected wind-driven PMSG system is modeled by solving the system differential equations using Runge-Kutta method by programming the m-file of MATLAB program. Three-phase-to-ground and single-phase-to-ground faults are applied at the connection bus between the PMSG wind farm and the 115-kV transmission line at t =30 s for a duration of 140ms (as the detection and operation times of the breakers extend to 140 ms) (Fischer de Toledo 2005). For comparison purpose the same faults are applied at the connection bus between the SCIG and DFIG wind farms and the 115-kV transmission line at t =30 s for a duration of 140ms and SCR of 16.

5.1 Grid-connected Wind-driven systems at fixed speed

The Grid-connected wind-driven systems of system in Fig. 6 are studied with fixed speed wind turbines at 10 m/s. The transient behaviour of systems before, during and after three-phase and single-phase to ground faults is studied.

The voltage and the frequency of PMSG are less than the rated voltage and rated frequency of wind farm (690V, 50Hz). Therefore, the converter and inverter are used to convert the voltage and frequency to rated values.

5.1.1 Three-phase-to-ground fault

A three phase to ground fault is applied at the connection bus (bus 3) between the wind farm and the 115-kV transmission line (Fig. 6a) at t =30 s for a duration of 140ms. Fig.7 shows the terminal voltage of the PMSG and the input dc voltage to DC-DC boost converter.

As shown in Fig. 7, the terminal voltage of PMSG before fault is 0.8 p.u (base 690 V) at a frequency of 40 Hz. During fault, the voltage collapses to zero at 30.25 sec with oscillations before recovering the pre-fault value. The pre-fault value of the input dc voltage to the converter is 568 V. During fault, the dc voltage reaches zero at 30.75 sec with oscillations before recovering its pre-fault value.

Figure 8 shows the temporal variations of the speed, voltage, active power and reactive power at Bus 1 for different wind farms.

As shown in Fig. 8, the time required of PMSG, SCIG and DFIG wind farms to recover their pre-fault values of speed,

voltage, active power and reactive power are approximately 0.25 sec, 1.5 sec and 1sec respectively. During fault, the speed of PMSG wind farm oscillates reaching 1.072p.u, against 1.032 p.u and 1.024 p.u for SCIG and DFIG wind farms, respectively. Also, the voltage of PMSG wind farm oscillates reaching 3 p.u, against 1.5 p.u and 1.1 p.u for SCIG and DFIG wind farms, respectively. This concludes that the performance of DFIG is better than SCIG under three-phase-to-ground fault conditions.

For SCIG, the pre-fault and post-fault values of the speed are equal to 1.015 p.u, which are almost of the same values as obtained previously using PSCAD simulator calculation (Fischer de Toledo 2005). During the fault, the speed reached 1.03 p.u against 1.06 p.u (Fischer de Toledo 2005). The voltage, the active power and the reactive power have the same trend during the fault as that reported before (Fischer de Toledo 2005). Generally, the mismatch between the previous and present calculations of the active and reactive power is nearly negligible and doesn't exceed 0.1%.

5.1.2 Single-phase-to-ground fault

A single phase to ground fault is applied at the connection bus between the wind farm and the 115-kV transmission line at t =30 s for a duration of 140ms. Fig. 9 shows the three phases terminal voltages of PMSG and the input dc voltage to DC-DC boost converter.

As shown in Fig. 9, the terminal voltage of PMSG before fault is 0.8 p.u (base 690 V) at a frequency of 40 Hz. During fault, the voltage of faulted phase (V_a) collapses to zero with oscillations before recovering the pre-fault value at 30.25 sec. The voltage of the other phases (V_b, V_c) decreases to 0.5 p.u with oscillations before recovering the pre-fault value at 30.25 sec. The pre-fault value of the input dc voltage to converter is 568 V. During fault, the voltage reaches to 250 V with oscillations before recovering the pre-fault value at 30.75 sec.

Figure.10 shows the temporal variations of the speed, voltage, active power and reactive power at Bus 1 for different wind farms.

As shown in Fig. 10, , the time required of PMSG, SCIG and DFIG wind farms to recover their pre-fault values of speed, voltage, active power and reactive power are approximately 0.25 sec, 1.0 sec and 0.5 sec, respectively. During fault, the speed of PMSG wind farm oscillates reaching 1.1p.u, against 1.02p.u and 1.005p.u for SCIG and DFIG wind farms, respectively.
The voltage of faulted phase (V_a) of PMSG, SCIG and DFIG wind farms decreases to zero while the other phase voltages (V_b and V_c) of PMSG oscillates reaching 1.01 p.u, against 1.3 p.u and 1.025 p.u for SCIG and DFIG wind farms, respectively. This concludes that the performance of DFIG is also better than SCIG under single-phase-to-ground fault conditions.

For SCIG, the pre-fault value of the speed is 1.015 p.u against 1.014 p.u using PSCAD simulator as reported before (Fischer de Toledo 2005). During the fault, the speed reached 1.018 p.u against 1.03 p.u before (Fischer de Toledo 2005). After the fault, the speed is 1.015 p.u against 1.02 p.u (Fischer de Toledo 2005). The pre-fault value of the voltage is 1.0 p.u which is almost of the same value as obtained previously using PSCAD simulator (Fischer de Toledo 2005). After the fault, the voltage decreased to 0.87 p.u (Fischer de Toledo 2005) against the constant voltage value of 1.0 p.u in the present calculation. The pre-fault and the post-fault values of the active and reactive power have the same trend as that reported before (Fischer de Toledo 2005) before, during and after the fault. Generally, the mismatch between the previous and present calculations of the active and reactive power is nearly negligible and doesn't exceed 0.1%.

5.2 Grid-connected Wind-driven systems at variable speed

The Grid-connected wind-driven systems of system in Fig. 6 are studied with variable speed wind turbines (Abdel-Salam 2011). The transient behaviour of systems before, during and after three-phase and single-phase to ground faults is studied. During fault, the voltage and the frequency of PMSG are less than the rated values of wind farm (690V, 50Hz).

5.2.1 Three-phase-to-ground fault

A three phase to ground fault is applied at the connection bus (bus 3) between the wind farm and the 115-kV transmission line at t =30 s for a duration of 140ms. Fig. 11 shows wind speed, the terminal voltage and frequency of PMSG and the input dc voltage to DC-DC boost converter.

As shown in Fig. 11, the terminal voltage of PMSG before fault changes between 0.6 to 1.2 p.u (base 690 V) at a frequency of 33 to 42 Hz when the wind speed changes from 8 to 12 m/sec. During fault, the voltage and frequency of PMSG collapse to zero with oscillations before recovering their pre-fault values at 30.25 sec. The input dc voltage to converter before fault

changes between 270 to 610 V. During fault, the dc voltage reaches zero with oscillations before recovering the pre-fault value at 30.75 sec.

Figure.12 shows the temporal variations of the speed, voltage, active power and reactive power at Bus 1.

As shown in Fig. 12, the speed of PMSG wind farm changes in the range 0.8 to 1.2 p.u against 0.65 to 1.065 p.u for DFIG wind farm. However, the speed of SCIG wind farm is 1p.u with spike at wind speed changes. Also, the voltage of PMSG wind farm is value 1 p.u, against 1.0 p.u and 1.05 p.u for SCIG and DFIG wind farms respectively. Moreover, the voltage of SCIG wind farm spikes at wind speed changes. The time required of PMSG, SCIG and DFIG wind farms to recover their pre-fault values of speed, voltage, active power and reactive power are approximately 0.25 sec, 1.5 sec and 1sec respectively. Again, the performance of DFIG is better than that of SCIG at varying wind speed.

5.2.2 Single-phase-to-ground fault

A single phase to ground fault is applied at the connection bus (bus 3) between the wind farm and the 115-kV transmission line at t =30 s for a duration of 140ms.

Fig. 13 shows the temporal variations of the speed, the voltage, the active power and the reactive power at Bus 1

As shown in Fig. 13, the speed of PMSG wind farm changes in the range 0.8 to 1.2 p.u against 0.65 to 1.065 p.u for DFIG wind farm. However, the speed of SCIG wind farm is 1p.u with small changes when wind speed changes. Also, the terminal voltage of PMSG wind farm is 1 p.u against 1.0 p.u and 1.05 p.u for SCIG and DFIG wind farms, respectively. However, the voltage of SCIG wind farm shows small change when wind speed changes. The times required of PMSG, SCIG and DFIG wind farms to recover their pre-fault values of speed, voltage, active power and reactive power are approximately 0.25 sec, 1.0 sec and 0.5 sec, respectively.

Different from SCIG, the PMSG and DFIG are not in need for a fixed capacitor to generate the active power, and the grid can easily feed the reactive losses of transmission lines and transformer at any value of SCR (SCR $\geq$ 1). This increases the dynamic stability of DFIG and PMSG when compared with SCIG. The active power of PMSG is 1 p.u compared to 0.87 p.u for DFIG and SCIG because some reactive power is absorbed by the IG to generate the active power.

The PMSG has the advantage of generating reactive power 0.43 p.u compared to the SCIG which is in shortage of the reactive power by 0.365p.u. On the other hand the DFIG absorbs zero reactive power, before fault (Mittal 2009).

During the fault, the speed of PMSG oscillates higher than DFIG and SCIG by approximately 10% due to flux oscillations required to feed the reactive power. This is because the speed is inversely proportional to flux (Hong-Woo 2010). Also, the PMSG has higher inertia being of larger weight when compared to DFIG and SCIG with a subsequent lower speed for PMSG (Mittal 2009).

Due to flux oscillations during fault, the voltage of PMSG oscillates to 3 p.u, which is higher than the corresponding voltages of DFIG and SCIG.

6. Conclusions

1) Different from SCIG, the PMSG and DFIG are not in need for a fixed capacitor to generate the active power, and the grid can easily feed the reactive losses of transmission lines and transformer at any value of SCR (SCR $\geq$ 1). This increases the dynamic stability of DFIG and PMSG when compared with SCIG.
2) During fault, the SCIG draws higher reactive power of -3.65p.u against -1.5p.u for the reactive power of DFIG and 0p.u for the reactive power of PMSG.
3) For the three-phase-to-ground fault, the time required to recover stability is approximately 0.25 sec for PMSG wind farm compared to 1 sec for DFIG wind farm and 1.5 sec for SCIG wind farm.
4) For the single-phase-to-ground fault, the time required to recover stability is approximately 0.25 sec for PMSG wind farm compared to 0.5 sec for DFIG wind farm and 1.0 sec for SCIG wind farm.
5) PMSG wind farm is more stable than DFIG and SCIG wind farms because the time required for PMSG wind farm to recover the stability is shorter than those of DFIG and SCIG wind farms for fixed and variable speeds.
6) The performance of DFIG is better than SCIG under three-phase-to-ground fault and single-phase-to-ground fault conditions.

7. Appendix

Detailed description of input data to model the system in MATLAB/SIMULINK

115 kV Transmission line data:

Length of line = 70 km

R_1 =0.0739 ohm/km, R_0 =0.388 ohm/km

X_{L1} =0.449 ohm/km, X_{L0} =1.522 ohm/km

X_{C1} =0.272 Mega ohm-km, X_{C0} =0.427 Mega ohm-km

Values: R_1, X_{L1}, R_0 and X_{L0} in ohm/km; X_{C1} and X_{C0} in Mega ohm-km

The SCIG:

Generator rating: 1.62 MVA (75 units)

Rated RMS line voltage: 690V

Stator resistance: 0.0025 p.u

Cage resistance: 0.0025 p.u

Stator unsaturated leakage reactance: 0.7 p.u

Mutual unsaturated reactance: 3.434

Rotor unsaturated mutual reactance: 0.7 p.u

Frequency: 50

No. of poles pair: 2

Reactive power compensation in the wind farm: 34 MVAr.

The DFIG

Generator rating: 1.62 MVA (75 units)

Rated RMS line voltage: 690V

Stator resistance: 0.0025 p.u

Rotor resistance: 0.0025 p.u

Stator unsaturated leakage reactance: 0.7 p.u

Mutual unsaturated reactance: 3.434

Rotor unsaturated mutual reactance: 0.7 p.u

Frequency: 50

No. of poles pair: 2

The PMSG:

Generator rating: 1.62 MVA (75 units)

Rated RMS line voltage: 690V

d-axis inductance : 0.7 p.u

q-axis inductance: 0.7 p.u

Rotor resistance: 0.0025 p.u

Frequency: 50

No. of poles pair: 4

Each Wind farm transformer:

Rating: 1.6 MVA

Winding voltages: 10.5/0.69

Leakage reactance: 0.0626

No-load losses and cooper losses: 0.0017 17 and 0.0002

Magnetizing current: 0.3 68

Step up transformer:

Rating: 150 MVA

Winding voltages: 10.5/115 kV

Leakage reactance: 0.06

No-load losses and cooper losses: 0.0017 and 0.0002

Magnetizing current: 0.3 68

Load connected at the end terminal of the line: 100 MW

System connected at the end terminal of the line:

Short Circuit Power: 2000 MVA, impedance angle 80°

References

Abbey, C., Khodabakhchian, B., Zhou, F., Dennetière, S., Mahseredjian, J., and Joos, G. (2005), "Transient Modeling and Comparison of Wind Generator Topologies", Paper No. IPST05, Presented at the International Conference on Power Systems Transients, June 19-23, Montreal, Canada.

Abdel-Salam, M., Ahmed, A. and Abdel-Sater, M. (2011), "Harmonic Mitigation, Maximum Power Point Tracking and Dynamic Performance of Variable Speed Grid Connected Wind Turbine", journal of Electric Power Component and Systems, Vol. 39, pp. 176-190.

Bhadra, SN., Kastha, D. and Banerjee, S. (2005), Wind electrical systems. Oxford: Oxford University, U.K.

Dusonchet, L. and Telaretti, E. (2011), "Effects of electrical and mechanical parameters on the transient voltage stabilityof a fixed speed wind turbine", Electric Power Systems Research, vol. 81, pp 1308–1316.

EL-Helw, H.M. and Tennakoon, S.B. (2008), "Evaluation of the suitability of a fixed speed wind turbine for large scale wind farms considering the new UK grid code", Renewable Energy, vol. 33, pp.1-12.

Fischer de Toledo, P. and Hailian, X. (2005), "WIND FARM IN WEAK GRIDS COMPENSATED WITH STATCOM". Proceedings of the Nordic wind power conference, Topic 7, Sweden.

Grainger, S.J. and Stevenson, W.D, Jr. (1994), "Power System Analysis", Book, McGraw-Hill, Inc.

Hong-Woo, K., Sung-Soo K. and Hee-Sang, K. (2010), "Modeling and control of PMSG-based variable-speed wind turbine", Electric Power Systems Research, vol. 80, pp 46–52.

Kesraoui, M., Bencherouda, O. and Mesbahi, Z., (2010), "Power Control of a PMSG based Wind Turbine System Above Rated Wind Speed", International Renewable Energy Congress, November 5-7, Sousse, Tunisia.

Mathworks (2008a) Inc. SimPowerSystems user's guide, version 7.6. USA: The Mathworks, Inc.

Mittal, R., Sandu, K.S. and Jain, D.K. (2008), "Power Conditioning of Variable Speed Driven PMSG for Wind Energy Conversion Systems", 2nd WSEAS/IASME International Conference on RENEWABLE ENERGY SOURCES (RES'08), October 26-28, Corfu, Greece.

Mittal, R., Sandu, K.S. and Jain, D.K. (2009), "Isolated Operation of Variable Speed Driven PMSG for Wind Energy Conversion System", IACSIT International Journal of Engineering and Technology, Vol. 1, No.3, August, pp 1793-8236.

Mohan, N., Undeland, T. and Robbins, W. (1989), "power electronics converters, application and design", Book, John wily and Sons, Inc.

Rahim, A.H.M.A. and Habiballah, I.O. (2011), "DFIG rotor voltage control for system dynamic performance enhancement", Electric Power Systems Research, vol. 81, pp 503–509.

Sermutlu, E. (2004), "COMPARISON OF RUNGE-KUTTA METHODS OF ORDER 4 AND 5 ON LORENZ EQUATION", Journal of Arts and Sciences, May.

Whei-Min, L., Chih-Ming, H., Ting-Chia, O. and Tai-Ming, C. (2011), " Hybrid intelligent control of PMSG wind generation system using pitch anglecontrol with RBFN", Energy Conversion and Management, vol. 52, pp1244–1251.

Zhanfeng, S., Changliang, X. and Tingna, S. (2010), "Assessing transient response of DFIG based wind turbines during voltage dips regarding main flux saturation and rotor deep-bar effect", Applied Energy, vol. 87, pp. 3283 – 3293.

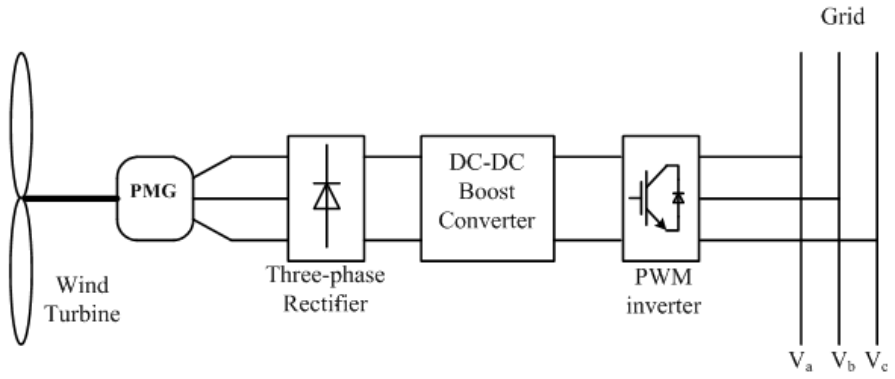

Figure 1. Grid-connected Wind-driven Permanent Magnet Synchronous Generator System

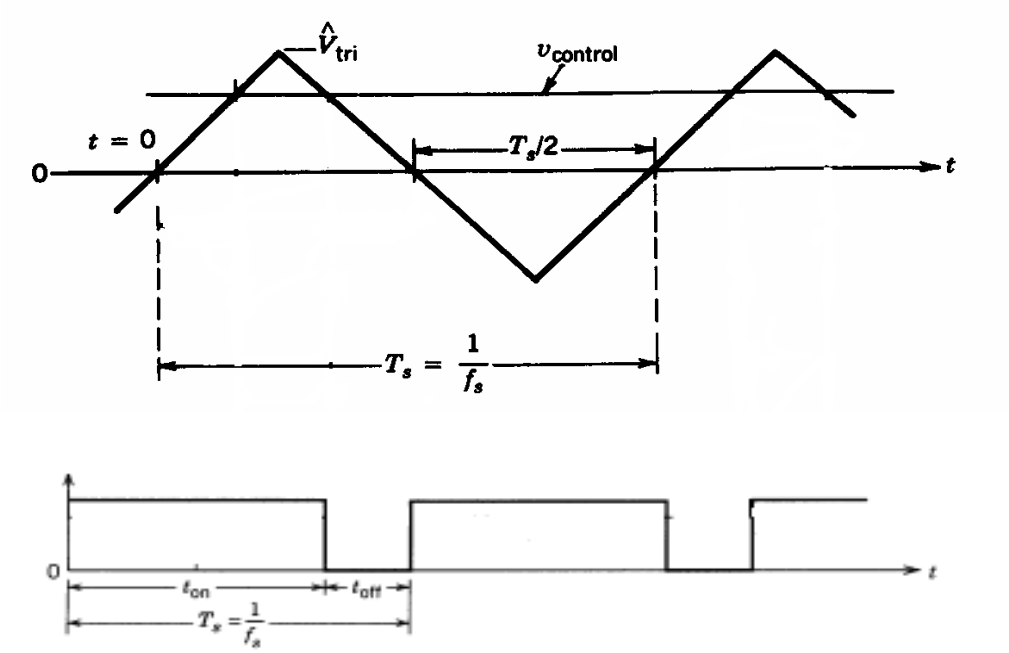

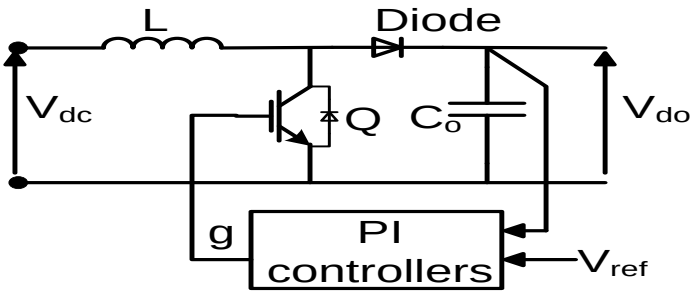

Figure 2. Switch mode DC-DC converter and DC-DC boost converter and its control

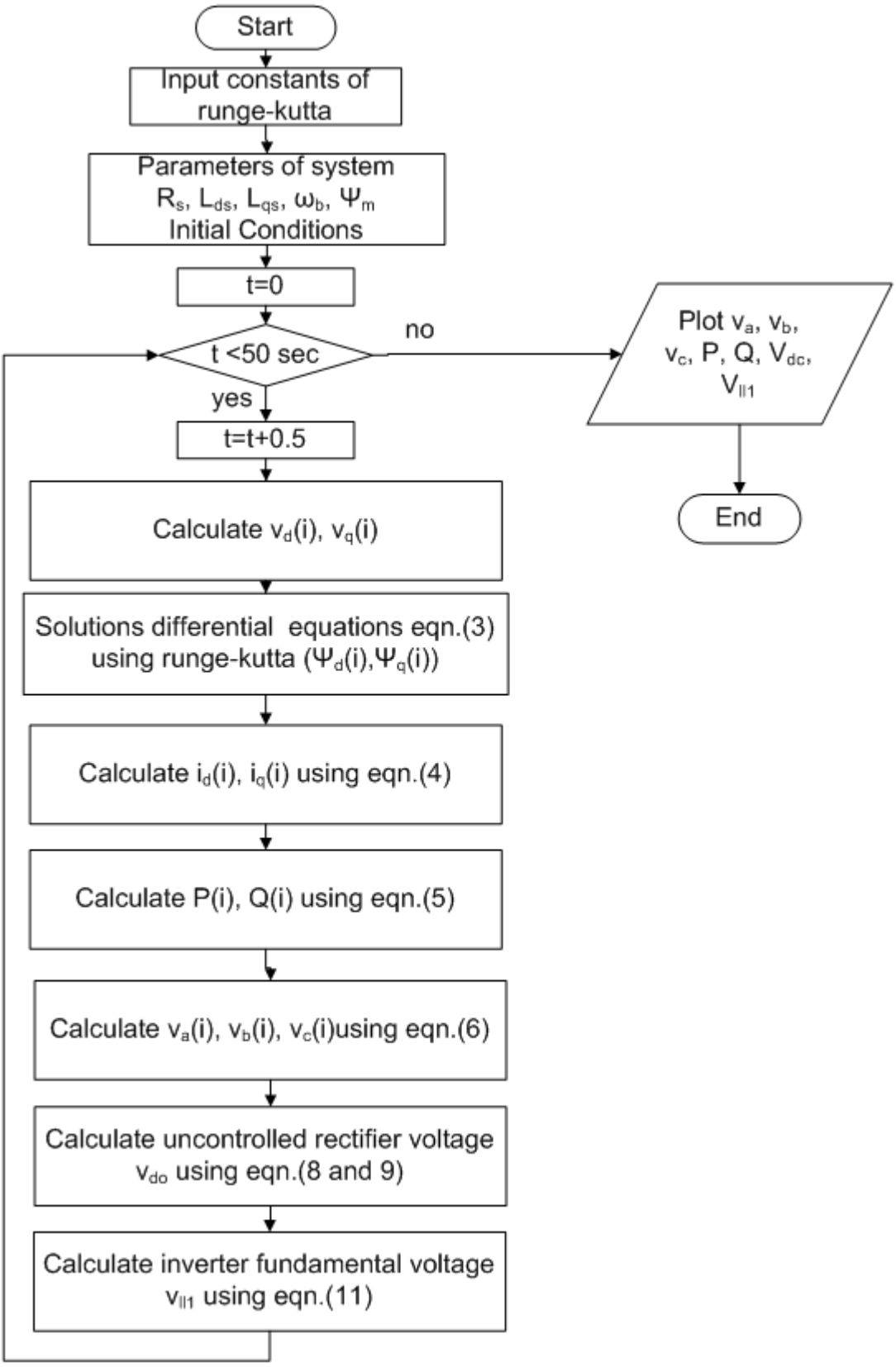
Start
Input constants of runge-kutta
Parameters of system
R_s, L_{ds}, L_{qs}, ω_b, Ψ_m
Initial Conditions
t=0
t <50 sec
no
yes
Plot v_a, v_b, v_c, P, Q, V_{dc}, V_{l1}
End
t=t+0.5
Calculate $v_d(i)$, $v_q(i)$
Solutions differential equations eqn.(3) using runge-kutta ($\Psi_d(i)$,$\Psi_q(i)$)
Calculate $i_d(i)$, $i_q(i)$ using eqn.(4)
Calculate P(i), Q(i) using eqn.(5)
Calculate $v_a(i)$, $v_b(i)$, $v_c(i)$using eqn.(6)
Calculate uncontrolled rectifier voltage v_{do} using eqn.(8 and 9)
Calculate inverter fundamental voltage v_{l1} using eqn.(11)

Figure 3. Flow chart of PMSG system modeling

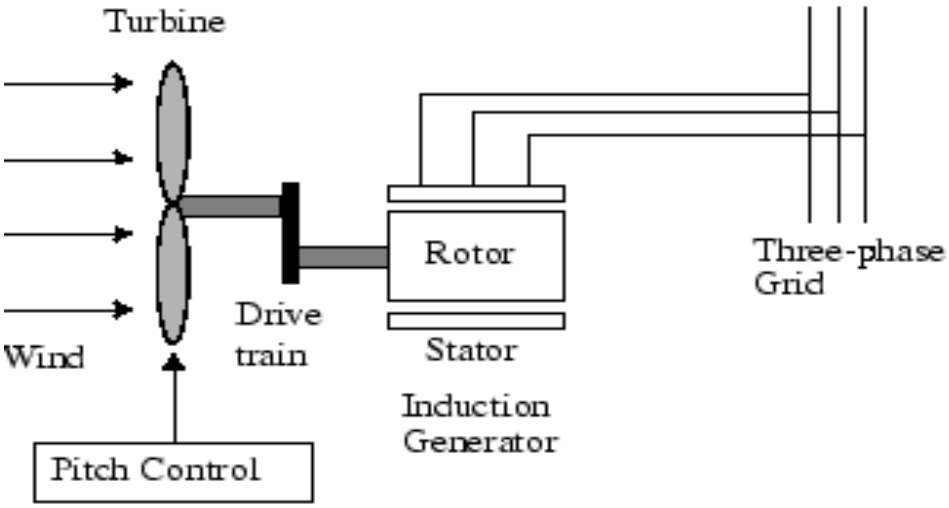

Figure 4. Grid-connected Wind-driven Squirrel Cage Induction Generator System

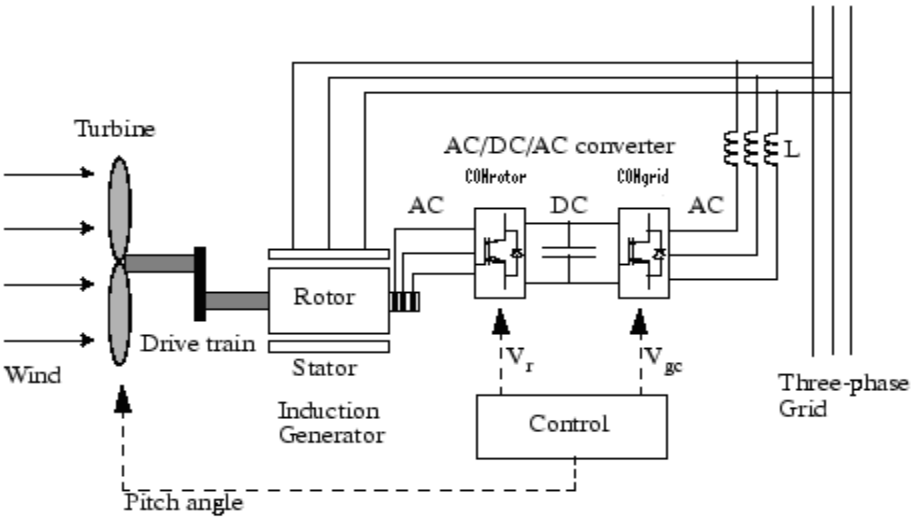

Figure 5. Grid-connected Wind-driven Doubly-Fed Induction Generator System

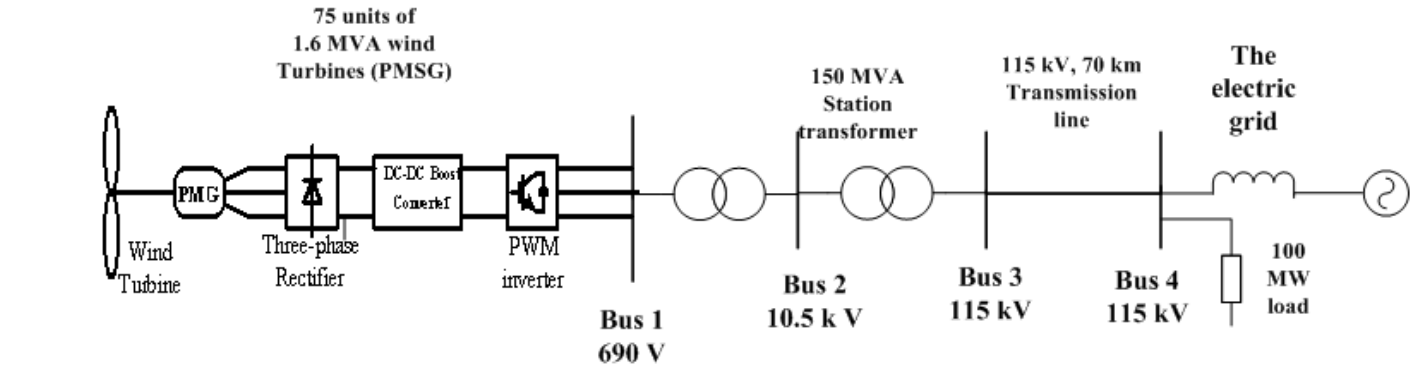

a. PMSG

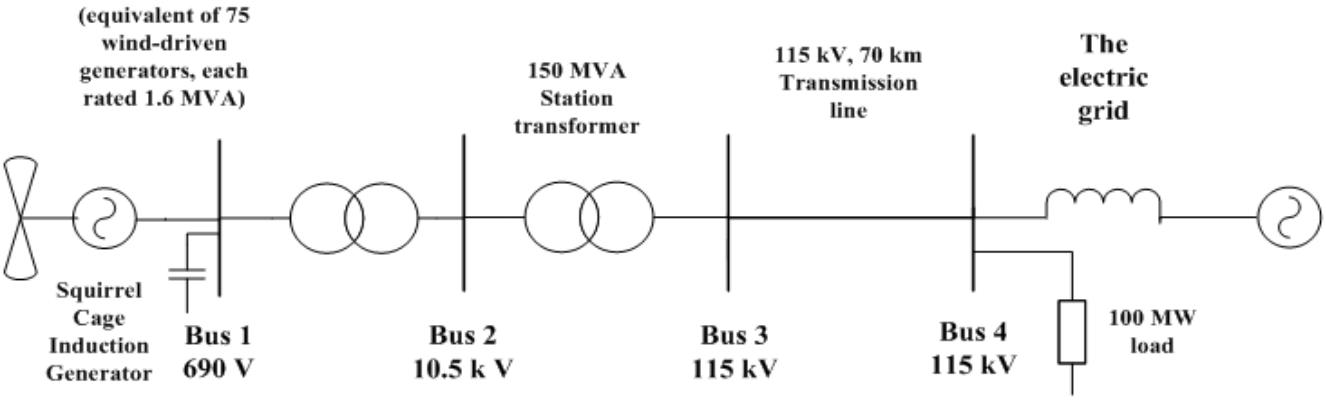

b. SCIG

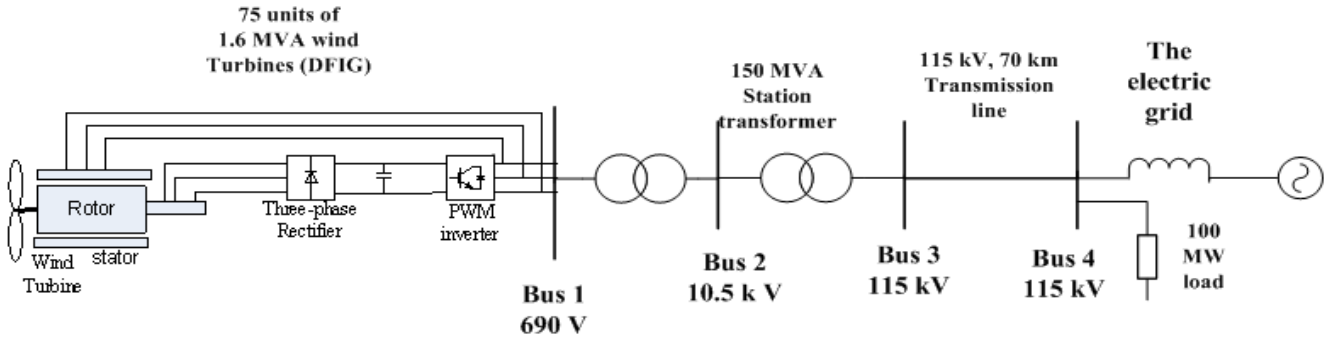

c. DFIG

Figure 6. Network model

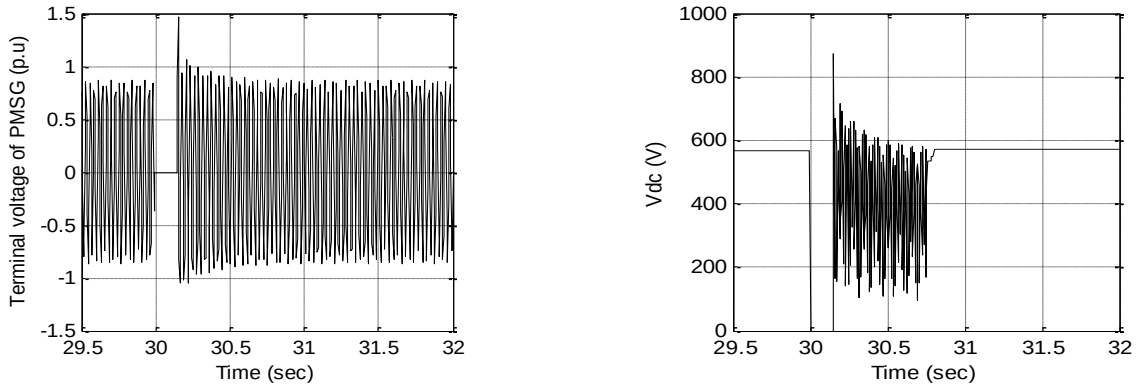

Figure 7. Terminal voltage of PMSG and dc voltage of converter.

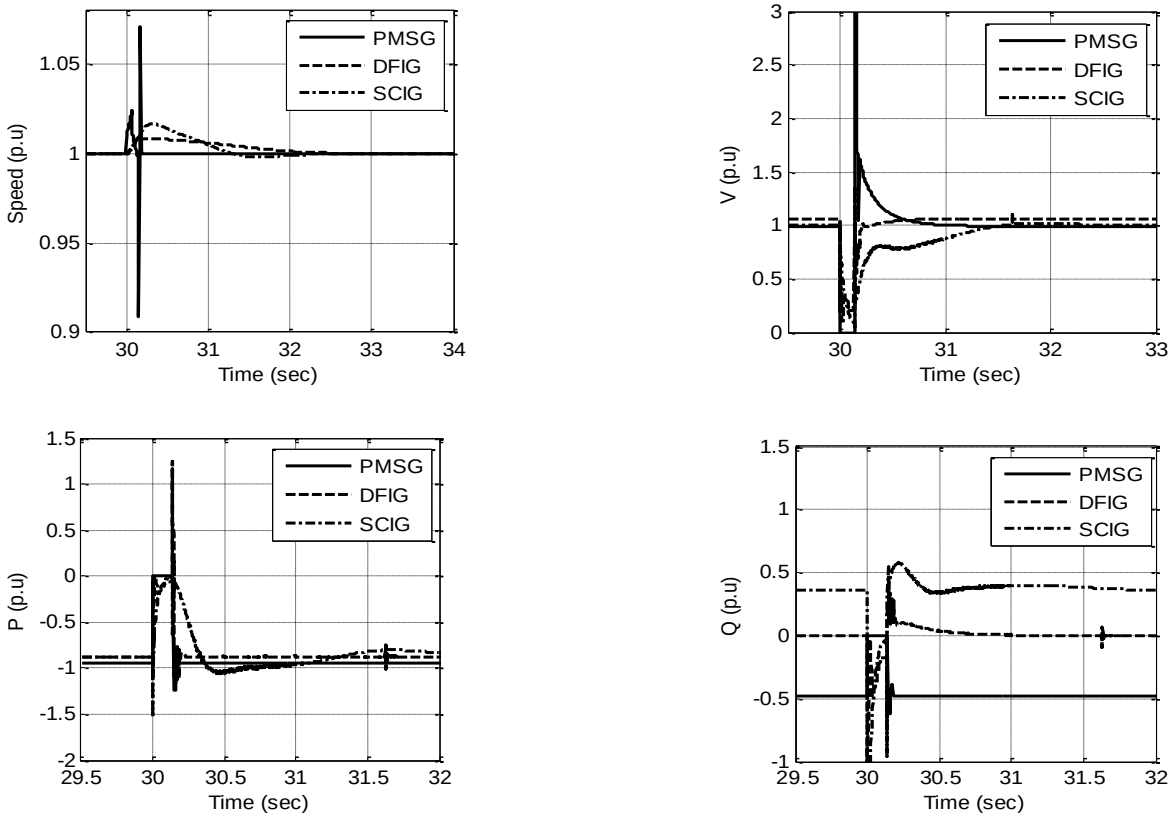

Figure 8. Temporal variations of the speed, the voltage, the active power and the reactive power at Bus 1 for different wind farms.

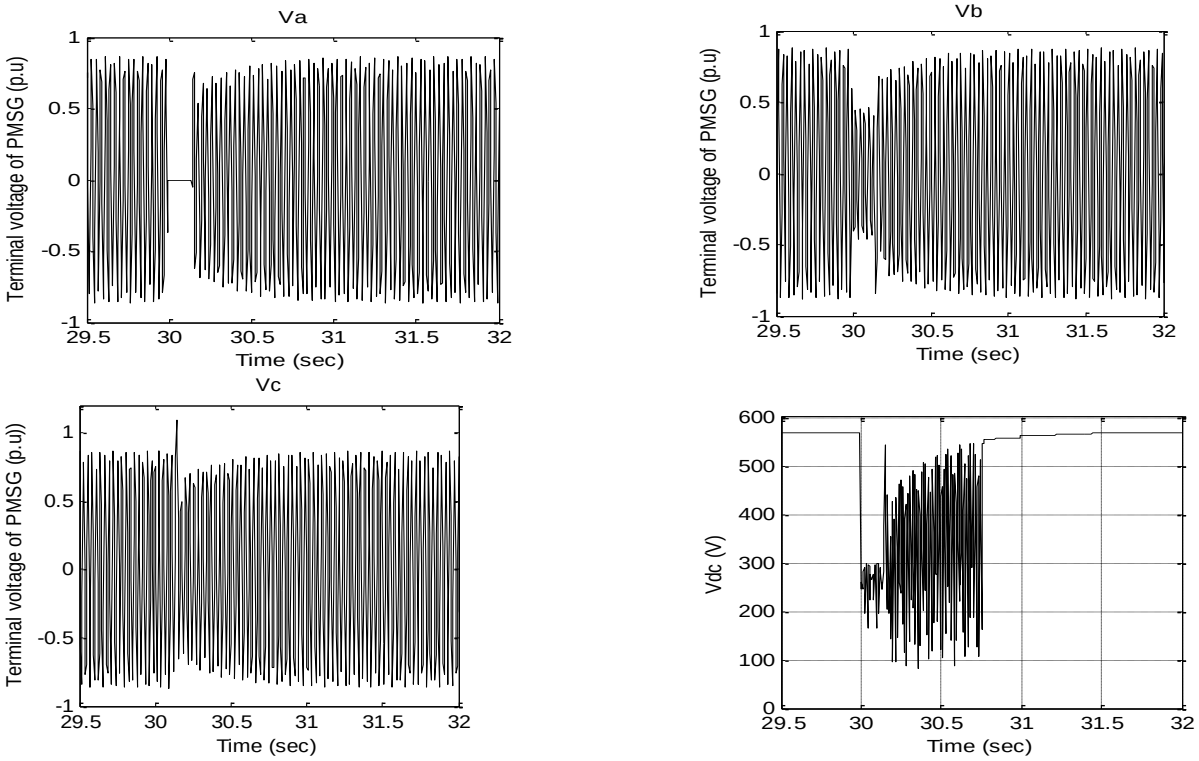

Figure 9. Three phases terminal voltages of PMSG and the input dc voltage to converter.

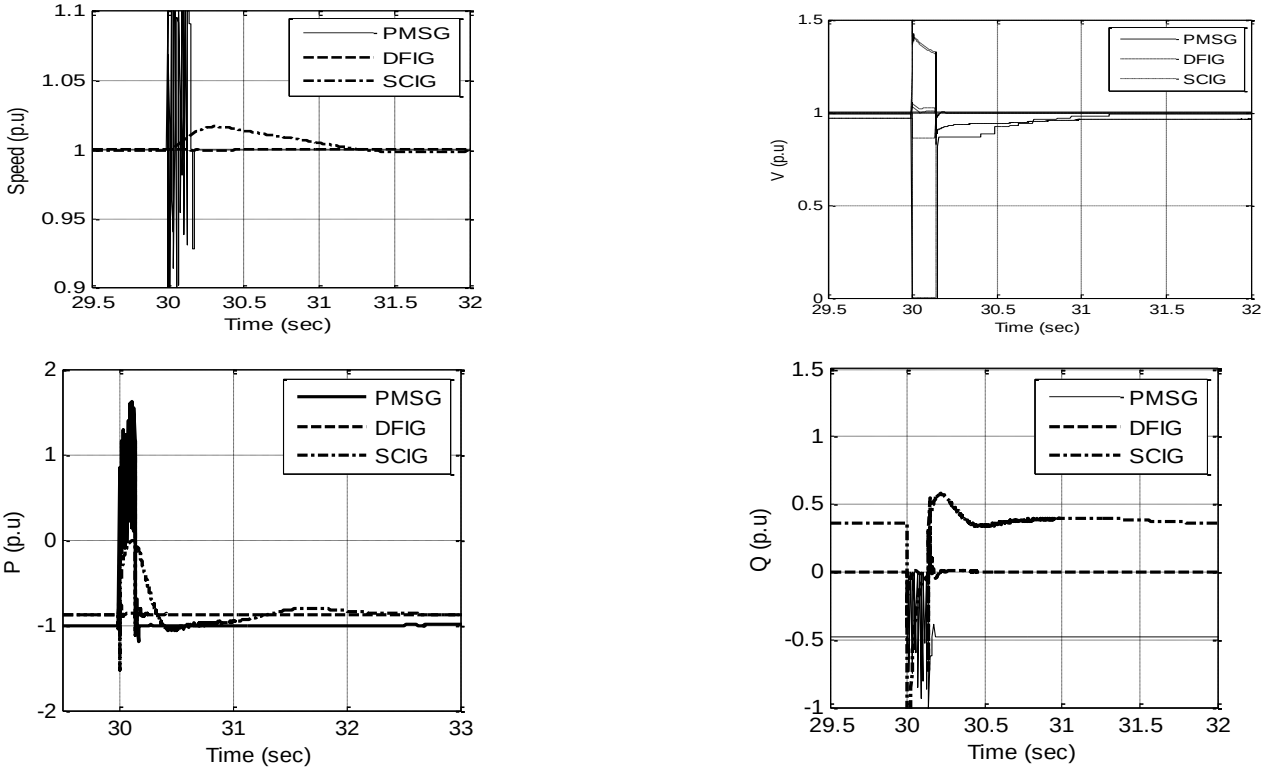

Figure 10. Temporal variations of the speed, the voltage, the active power and the reactive power at Bus 1 for different wind farm

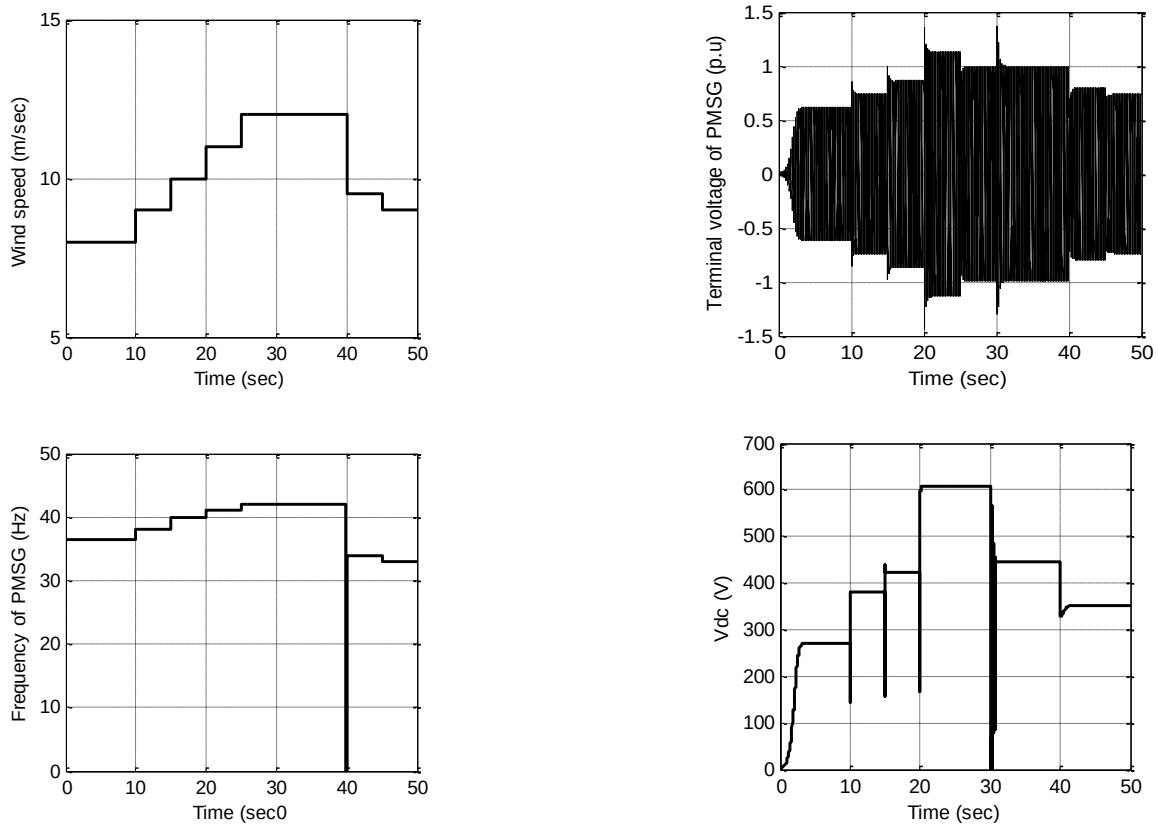

Figure 11. Wind speed, the terminal voltage and frequency of PMSG and the input dc voltage to converter.

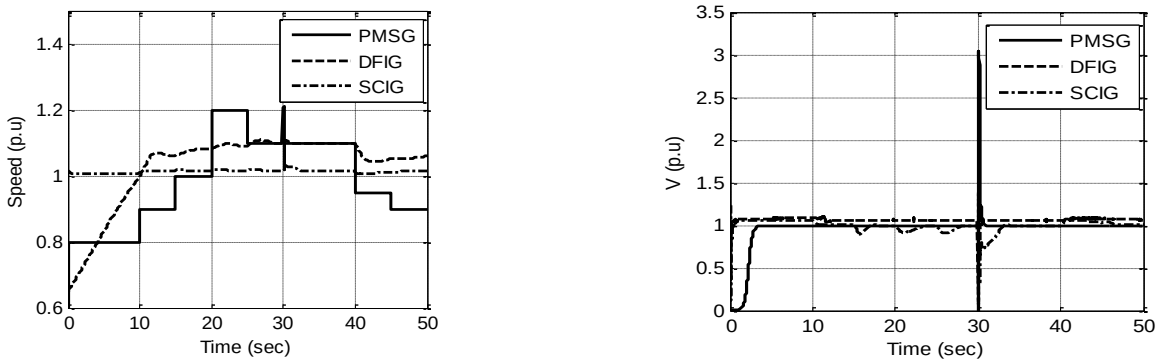

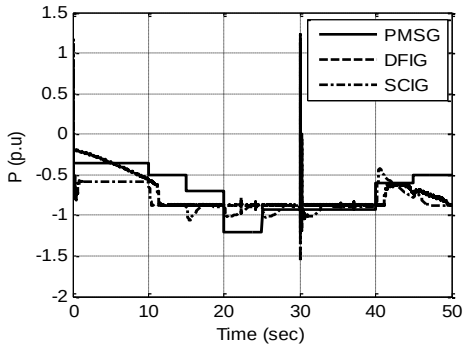

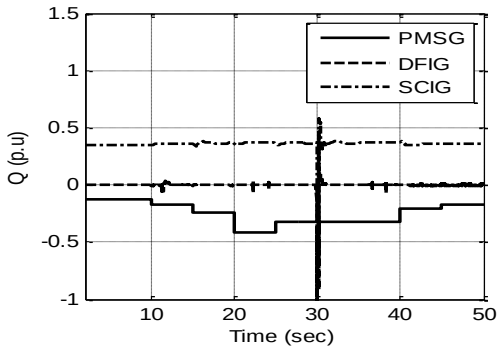

Figure 12. Temporal variations of the speed, voltage, active power and reactive power at Bus 1

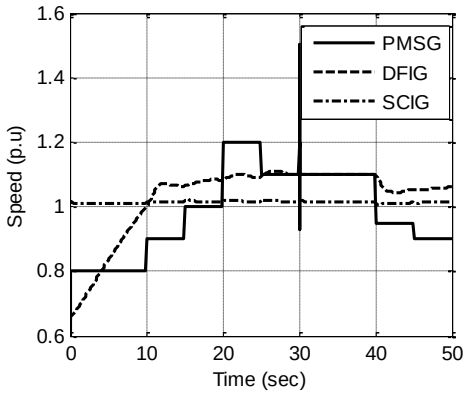

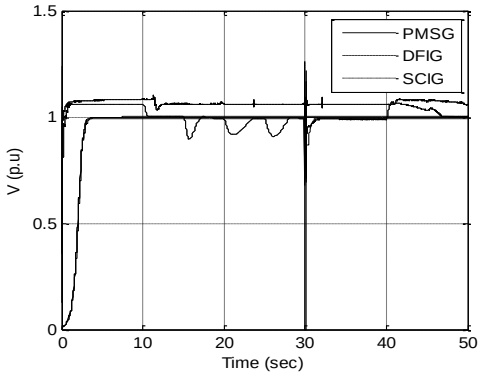

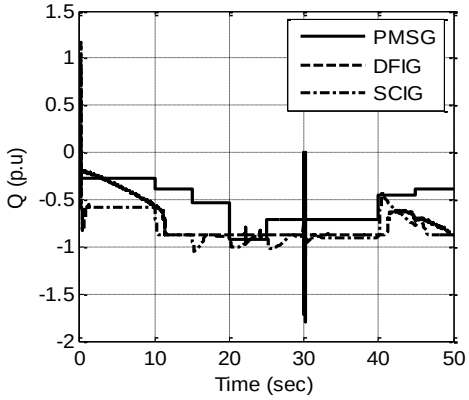

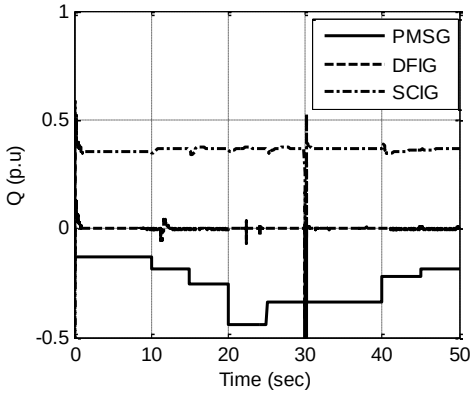

Figure 13. Temporal variations of the speed, the voltage, the active power and the reactive power at Bus 1